ARTICLE

doi:10.1038/nature11162

NPR3 and NPR4 are receptors for the immune signal salicylic acid in plants

Zheng Qing Fu[1]*, Shunping Yan[1]*, Abdelaty Saleh[1]*, Wei Wang[1], James Ruble[2], Nodoka Oka[3], Rajinikanth Mohan[1], Steven H. Spoel[4], Yasuomi Tada[5], Ning Zheng[2] & Xinnian Dong[1]

Salicylic acid (SA) is a plant immune signal produced after pathogen challenge to induce systemic acquired resistance. It is the only major plant hormone for which the receptor has not been firmly identified. Systemic acquired resistance in *Arabidopsis* requires the transcription cofactor nonexpresser of PR genes 1 (NPR1), the degradation of which acts as a molecular switch. Here we show that the NPR1 paralogues NPR3 and NPR4 are SA receptors that bind SA with different affinities. NPR3 and NPR4 function as adaptors of the Cullin 3 ubiquitin E3 ligase to mediate NPR1 degradation in an SA-regulated manner. Accordingly, the *Arabidopsis npr3 npr4* double mutant accumulates higher levels of NPR1, and is insensitive to induction of systemic acquired resistance. Moreover, this mutant is defective in pathogen effector-triggered programmed cell death and immunity. Our study reveals the mechanism of SA perception in determining cell death and survival in response to pathogen challenge.

After pathogen challenge, host cells have to make a life-and-death decision to fend off infection. Recognition of a pathogen effector by a host resistance protein can lead to effector-triggered immunity (ETI), characterized by rapid programmed cell death (PCD) known as the hypersensitive response[1]. The clearly defined boundary of the hypersensitive response indicates the presence of a mechanism that controls cell death and survival. Despite intense studies of plant mutants defective in controlling the spread of PCD[2], the regulatory mechanism still remains a mystery.

Localized PCD can induce systemic acquired resistance (SAR) through the production of the immune signal, salicylic acid (SA)[3]. SA triggers global transcriptional reprogramming and resistance to a broad spectrum of pathogens. The receptor for SA has been sought after for many years, mainly through biochemical purification of SA-binding proteins[4–6]. However, genetic data for these SA-binding proteins, which include a catalase, a chloroplast carbonic anhydrase, and a methyl SA esterase, suggest that none of them functions as a bona fide SA receptor. By contrast, genetic studies of SA-insensitive mutants have strongly suggested that NPR1, which contains a BTB (bric à brac, tramtrack, broad-complex) domain, an ankryin repeat domain and a nuclear localization sequence, is a potential SA receptor[7]. However, the NPR1 protein does not have considerable SA binding activity under different test conditions (Supplementary Fig. 2).

Instead of direct binding, SA has been shown to control the nuclear translocation of NPR1 through cellular redox changes[8]. In the absence of pathogen challenge, NPR1 is retained in the cytoplasm as an oligomer through redox-sensitive intermolecular disulphide bonds. After induction, these disulphide bonds are reduced, releasing NPR1 monomers into the nucleus, where NPR1 acts as a cofactor for transcription factors, such as TGAs, to induce defence-related genes. In the absence of a functional NPR1 protein, SA-induced transcriptional reprogramming is almost completely blocked.

The presence of a BTB domain in NPR1 suggests that, like other BTB domain-containing proteins, it may interact with Cullin 3 (CUL3) E3 ligase and mediate substrate degradation[9]. However, our research led to the surprising finding that the NPR1 protein itself is degraded by the proteasome. Although NPR1 is degraded in the nucleus of resting cells to dampen basal expression of defence genes, it is phosphorylated after immune activation at an IκB-like phosphodegron motif, ubiquitinylated by a CUL3 E3 ligase, and degraded to sustain maximum levels of target gene expression probably through accelerated recycling of the transcription initiation complex[10]. Blocking NPR1 degradation by mutating the IκB-like phophodegron in NPR1 or the two *CUL3* genes (*cul3a cul3b*) in *Arabidopsis* led to increased basal resistance, but insensitivity to SAR induction. Therefore, nuclear accumulation of NPR1 is needed for basal defence gene expression and resistance, whereas its subsequent turnover is required for establishing SAR.

NPR3 and NPR4 are CUL3 adaptors for NPR1 degradation

In a search for the adaptor proteins of the CUL3 E3 ligase that specifically target NPR1 for degradation, we considered its paralogues, NPR3 and NPR4, as possible candidates, because both contain the BTB domain as well as an extra protein–protein interaction domain (ankyrin repeat) (Supplementary Fig. 3), which are typical for CUL3 substrate adaptors[9]. More importantly, despite their sequence similarities to NPR1, the *npr3 npr4* double mutant has the opposite phenotype of *npr1* in that it exhibits enhanced disease resistance[11], a phenotype reminiscent of the *cul3a cul3b* mutant[10].

To test our hypothesis that NPR3 and NPR4 are CUL3 adaptors for NPR1 degradation, we examined the accumulation of NPR1 protein in wild-type, *npr3*, *npr4* and *npr3 npr4* mutant plants. NPR1 protein levels were higher in the *npr4* and *npr3 npr4* mutants than in the wild type in the absence of exogenous SA, and increased faster in the *npr3*, *npr4* and *npr3 npr4* mutants compared with wild type in response to SA treatment (Fig. 1a). The effects of *npr3* and *npr4* on NPR1 were probably post-transcriptional, as *NPR1* transcripts were not increased in these mutants (Supplementary Fig. 4). To prove our hypothesis

[1]Howard Hughes Medical Institute–Gordon and Betty Moore Foundation, Department of Biology, PO Box 90338, Duke University, Durham, North Carolina 27708, USA. [2]Howard Hughes Medical Institute, Department of Pharmacology, University of Washington, PO Box 357280, Seattle, Washington 98195, USA. [3]Faculty of Agriculture, Kagawa University, Miki, Kagawa 761-0795, Japan. [4]Institute of Molecular Plant Sciences, University of Edinburgh, Edinburgh EH9 3JR, UK. [5]Life Science Research Center, Institute of Research Promotion, Kagawa University, 2393 Ikenobe, Miki-cho, Kita-gun, Kagawa 761-0795, Japan.
*These authors contributed equally to this work.

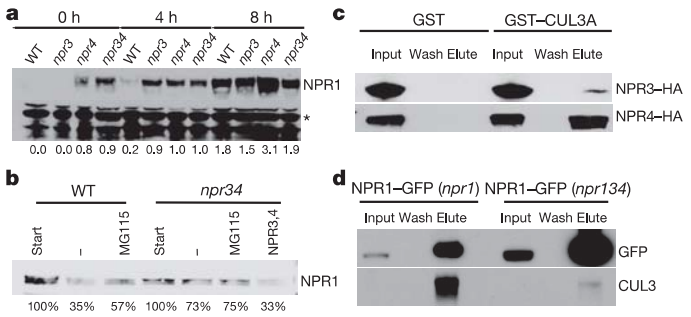

Figure 1 | NPR3 and NPR4 mediate degradation of NPR1. **a**, NPR1 protein levels in wild type (WT), *npr3*, *npr4* and *npr3 npr4* (*npr34*) plants treated with 0.5 mM SA. The NPR1 level (shown at bottom) was determined on the basis of the ratio of the NPR1 band intensity to that of the non-specific band (asterisk). **b**, GST–NPR1 degradation in extracts from wild-type or *npr3 npr4* double mutant (*npr34*), with or without (−) MG115 or with recombinant His–MBP–NPR3 and His–MBP–NPR4 proteins (NPR3,4). **c**, *In vitro* pull-down assay of GST–CUL3A and NPR3–HA and NPR4–HA. **d**, Co-immunoprecipitation of NPR1–GFP and CUL3 in *npr1* and *npr1 npr3 npr4* (*npr134*) plants.

further, we performed *in vitro* degradation experiments using purified recombinant glutathione *S*-transferase (GST)-tagged NPR1 protein. We found that after 15 min of incubation, the recombinant NPR1 protein was degraded in the wild-type plant extract, but not in *npr3 npr4* (Fig. 1b). The addition of purified recombinant NPR3 and NPR4 proteins tagged with histidine (His) and maltose binding protein (MBP) to the extract complemented the mutant phenotype, supporting a role of NPR3 and NPR4 in mediating NPR1 degradation. This degradation is probably through the proteasome, as application of the proteasome inhibitor MG115 stabilized the protein (Fig. 1b). To demonstrate further that NPR3 and NPR4 act as adaptors for the CUL3 E3 ligase, we first performed pull-down experiments using *in vitro* translated haemagglutinin (HA)-tagged NPR3 (NPR3–HA) and NPR4–HA. We found that CUL3A could pull down NPR3 and NPR4, with NPR4 showing a stronger interaction (Fig. 1c). Then we performed a co-immunoprecipitation assay using transgenic plants constitutively expressing NPR1–green fluorescent protein (GFP) in *npr1* and *npr1 npr3 npr4* mutants. We found that the amount of the endogenous CUL3 protein pulled down by NPR1–GFP was significantly reduced in the *npr1 npr3 npr4* triple mutant compared with the *npr1* single mutant (Fig. 1d), indicating that the NPR1–GFP interaction with CUL3 requires NPR3 and NPR4. These results further support our hypothesis that NPR4 and NPR3 are CUL3 adaptors for the degradation of NPR1 before and after SA induction, respectively (Fig. 1a).

SA affects NPR1–NPR3 and NPR1–NPR4 interactions

Proteasome-mediated protein degradation has a crucial role in regulating plant hormone receptors[12]. In some of these cases, the hormones act as a molecular glue to enable the formation of the receptor complex[13,14], which includes the substrate adaptor for the E3 ligase and the corresponding substrate. Our data show that proteasome-mediated degradation of NPR1 is also involved in SA signalling[10], although a different E3 ligase (CUL3, instead of CUL1) is used.

To test the possibility that SA is part of the NPR1–NPR3/4 complex, we performed a yeast two-hybrid (Y2H) assay. Using NPR3 as bait and NPR1 as prey, little growth was observed on plates without SA (Fig. 2a). However, yeast growth was observed on plates supplemented with 100 μM SA or with the functional analogue of SA 2,6-dichloroisonicotinic acid (INA)[15], but not on plates with 4-hydroxybenzoic acid (4-HBA)[6], which cannot induce SAR. Interestingly, although SA promoted the NPR1–NPR3 interaction, it disrupted the interaction between NPR1 and NPR4 (Fig. 2b). Moreover, NPR3 and NPR4 could form both homodimers and heterodimers with each other in the presence of SA and INA, but not 4-HBA (Fig. 2c). This suggests that NPR3 and

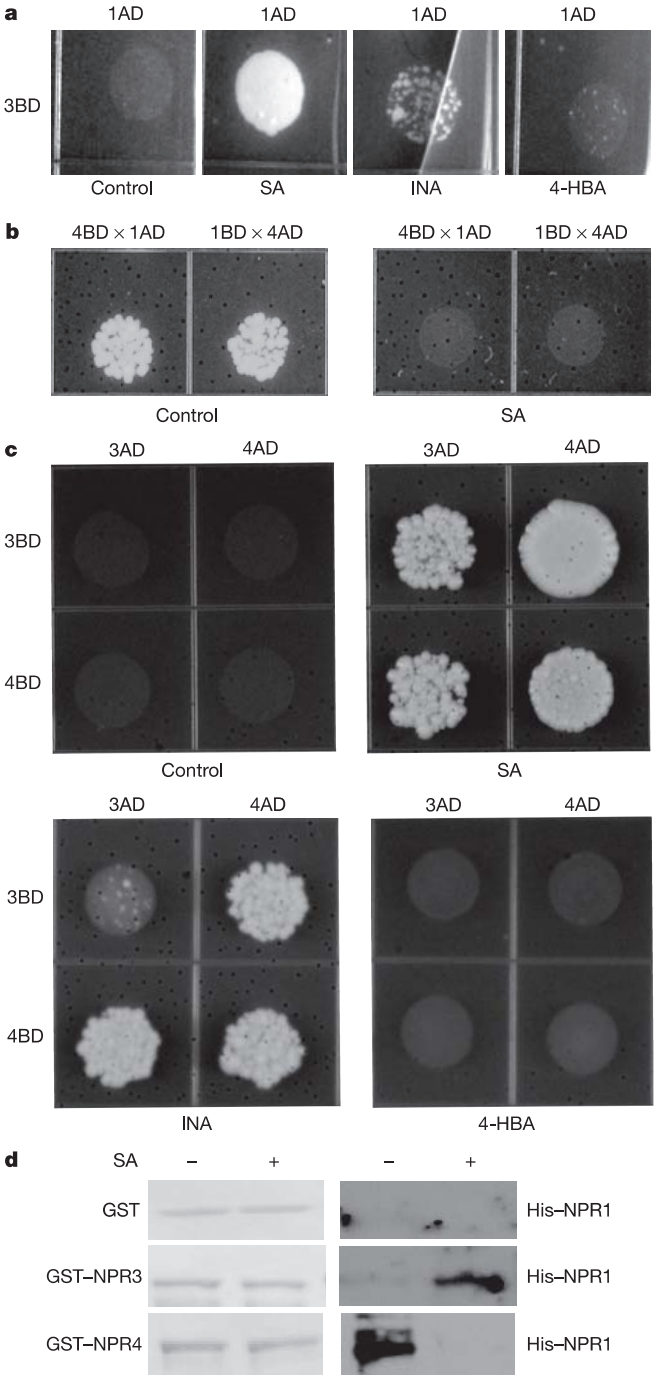

Figure 2 | SA directly regulates interactions between NPR proteins. **a–c**, Yeast two-hybrid assay to test interactions between NPR1 and NPR3 (**a**), NPR1 and NPR4 (**b**), and NPR3 and NPR4 (**c**). Diploid yeast cells were spotted on plates (SD media lacking Trp, Leu and His, plus 3 mM 3-aminotriazole) without (control) or with 100 μM SA, INA or 4-HBA. AD, activation domain; BD, DNA-binding domain. 1, NPR1; 3, NPR3; 4, NPR4. **d**, *In vitro* pull-down assays between His–MBP–NPR1 and GST–NPR3 and GST–NPR4 in the presence or absence of 100 μM SA.

NPR4 not only control NPR1 stability, but also self-regulate. Because NPR1 did not form homodimers with or without SA and interacted with NPR2 independently of SA (Supplementary Fig. 5), we focused on the regulatory roles of NPR3 and NPR4.

To validate the Y2H data further, we performed *in vitro* pull-down assay. As shown in Fig. 2d, using the GST–NPR3 protein, we were able to pull down His–MBP–NPR1 only in the presence of SA. By contrast, GST–NPR4 could pull down His–MBP–NPR1 only in the absence of SA, indicating that the NPR1–NPR4 interaction was disrupted by SA.

NPR3 and NPR4 bind SA with different affinities

Both the Y2H and the *in vitro* pull-down results strongly suggest that SA directly binds to NPR3 and NPR4 to control their interactions with NPR1. To prove that NPR3 and NPR4 are SA receptors, we measured their SA-binding activities using [^{3}H]-SA. We found that both GST-tagged NPR3 and NPR4 recombinant proteins bound [^{3}H]-SA (Fig. 3a, b and Supplementary Fig. 2a). Next, we assessed whether active or inactive SA analogues could compete with [^{3}H]-SA to bind to GST–NPR3 and GST–NPR4. The active SAR inducer 5-chlorosalicylic acid[6] and INA reduced the binding of [^{3}H]-SA to GST–NPR3 and GST–NPR4, whereas 4-HBA had little effect (Fig. 3a, b). To assess the binding affinity of NPR3 and NPR4, we performed saturation binding experiments. Whereas NPR4 had a classical saturation curve (Fig. 3c), NPR3 binding could not be saturated even with 1,000 nM [^{3}H]-SA, indicating that NPR3 has a lower affinity than NPR4. Accordingly, the binding of SA to NPR3 was slower than NPR4 (Supplementary Fig. 6). Next, we analysed the saturation binding data with GraphPad Prism using different models, and found that the model 'one site—specific binding with Hill slope' is significantly better than the other models, which indicates that there are several binding sites or fractions in NPR3 and NPR4. The dissociation constant (K_d) for NPR4 was 46.2 ± 2.35 nM (mean ± s.e.m.) with a Hill coefficient (h) of 0.830 ± 0.0314. To check the cooperativity of different binding sites, we carried out dissociation experiments by the addition of 1 mM non-radioactive-labelled SA (cold SA) or by infinite dilution. The dissociation curves (Fig. 3d) indicate that NPR4 has several SA-binding sites, and the lack of overlap between the two curves suggests negative cooperativity between these binding sites (the first binding reduces the affinity for subsequent binding). The K_d value for NPR3 (981 nM, Supplementary Fig. 7) was significantly higher than 100 nM, which made saturation binding an inappropriate way to calculate the K_d. Therefore, we performed a homologous competitive binding assay (Fig. 3e). The half-maximum inhibitory concentration (IC_{50}) was calculated to be 1,811 nM ($\log(IC_{50}) = 3.26 \pm 0.0901$) with a Hill coefficient of 0.554 ± 0.0612. Through these analyses, we demonstrated that NPR3 and NPR4 bind SA specifically and with different affinities.

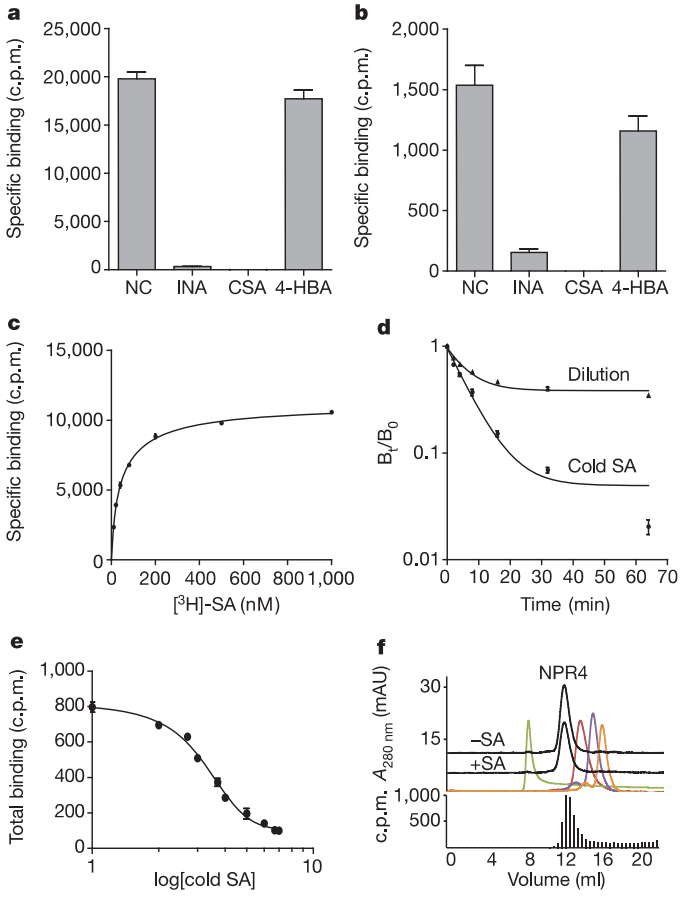

Figure 3 | NPR3 and NPR4 bind SA. **a**, **b**, Competition binding assay of NPR4 (**a**) and NPR3 (**b**). c.p.m., counts per minute; CSA, 5-chlorosalicylic acid; NC, no competitor. **c**, Saturation binding assay of NPR4. $K_d = 46.2 \pm 2.35$ nM, $h = 0.830 \pm 0.0314$. **d**, Dissociation assay of NPR4. The dissociation was initiated by the addition of 1 mM non-radioactive-labelled SA (cold SA) or by infinite dilution. B_0 and B_t are total binding before and after dissociation, respectively. **e**, Homologous competitive binding assay of NPR3. $IC_{50} = 1{,}811$ nM ($\log(IC_{50}) = 3.26 \pm 0.0901$), $h = 0.554 \pm 0.0612$. **f**, Size exclusion chromatography showing that NPR4 tetramer binds SA (black). Top panel, elution profile. Green, red, purple and orange peaks correspond to 2,000, 158, 75 and 44 kDa, respectively. Bottom panel, total binding of [^{3}H]-SA in different fractions. mAU, milli-absorbance units. Error bars represent s.d. ($n = 2$ or 3).

To examine the receptor complex further, we performed gel filtration analysis on the purified recombinant NPR4 protein—the receptor with the higher affinity to SA. Because the recombinant NPR4 protein spontaneously oligomerized *in vitro* in the absence of a reducing agent, our analysis focused on samples pretreated with 100 mM dithiothreitol (DTT) followed by dialysis against 5 mM DTT. We discovered that NPR4 was present in an estimated tetrameric form, which was competent in binding to SA (Fig. 3f). Notably, SA binding did not change the gel filtration elution profile of the protein. Further experiments are required to investigate how SA affects the receptor complexes to make them either more accessible (that is, NPR3 binding to NPR1) or less accessible (that is, NPR4 binding to NPR1) for substrate binding.

The *npr3 npr4* double mutant is defective in SAR and ETI

To understand the biological significance of NPR3/4-mediated degradation of NPR1, a positive regulator of SAR, we first performed SAR tests in the *npr3*, *npr4* and *npr3 npr4* mutants using *Pseudomonas syringae* pv. *maculicola* ES4326 (*Psm* ES4326). Consistent with a previous report[11], there was a significant reduction in *Psm* ES4326 growth in the *npr3 npr4* double mutant without SAR induction (Fig. 4a). However, even after SAR induction by local inoculation of avirulent *Psm* ES4326/*avrRpt2*, no further reduction in growth of virulent *Psm* ES4326 in systemic tissue was observed in the *npr3 npr4* double mutant. To a lesser degree, SAR was also defective in the *npr3* single mutant. Thus, stabilization of NPR1 protein in the *npr3* and *npr3 npr4* mutants rendered these plants insensitive to SAR induction. This phenotype is similar to that observed in the *cul3a cul3b* double mutant[10], validating the role of NPR3 and NPR4 in CUL3-mediated degradation of NPR1 and SAR.

On the basis of our knowledge that SAR and ETI are two distinct defence strategies, with the former promoting cell survival and the latter triggering PCD, we then tested the *npr* mutants for ETI using *Pseudomonas* strains expressing different effectors. Surprisingly, we found that the *npr3 npr4* mutant failed to undergo PCD (Fig. 4b and Supplementary Fig. 8a) as quantified by ion leakage (Fig. 4c), and was compromised in resistance triggered by the effectors (Fig. 4d). The same phenotypes were observed in different mutant alleles of *npr3*, *npr4* and *npr3 npr4* (Supplementary Fig. 8b). The ETI deficiency observed in *npr3 npr4* is probably caused by the increased accumulation of NPR1, because this phenotype was suppressed in the *npr1 npr3 npr4* triple mutant.

To observe NPR1 turnover in response to pathogen challenge *in situ*, we inoculated *Psm* ES4326/*avrRpt2* in the *35S:NPR1(C82A)-GFP* transgenic plant, in which NPR1 is constitutively localized in the nucleus (Fig. 4e)[16]. Eleven hours after inoculation, some cells showed increased chlorophyll leakage (Fig. 4f, red) with overlapping accumulation of phenolic compounds (Fig. 4e, larger green spots) indicative of PCD (Fig. 4g, yellow), whereas other cells were still intact. The NPR1(C82A)–GFP fluorescence was markedly reduced inside the inoculated region (Fig. 4g, h). Notably, the NPR1(C82A)–GFP fluorescence level was the highest in the cells surrounding the hypersensitive

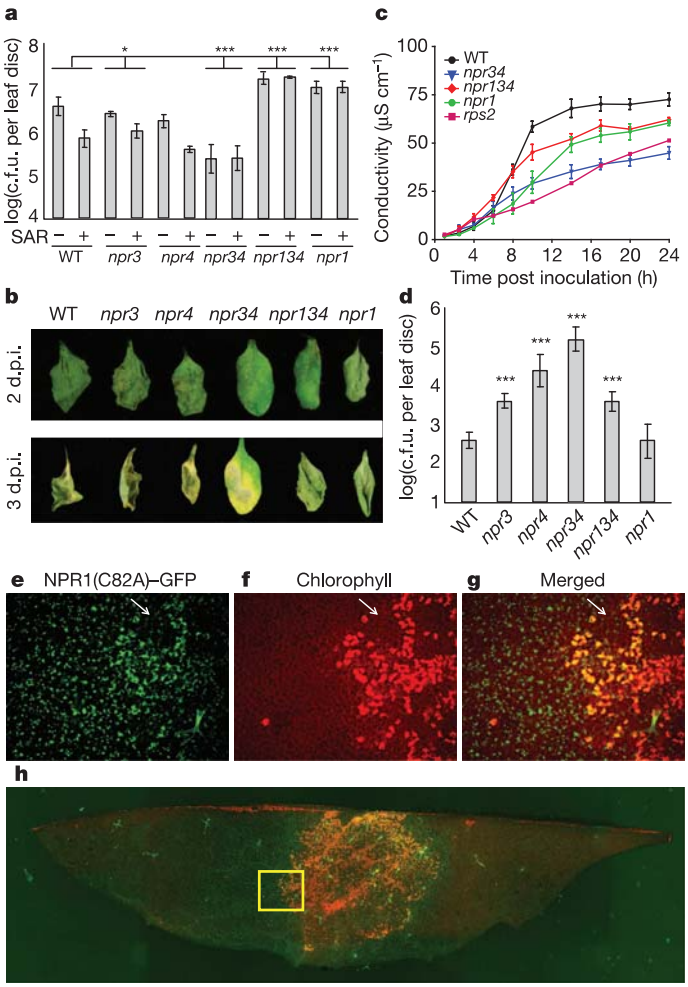

Figure 4 | SA receptors control NPR1 stability to regulate SAR and ETI. **a**, SAR test in wild-type, *npr3*, *npr4*, *npr3 npr4* (*npr34*), *npr1 npr3 npr4* (*npr134*) and *npr1*. c.f.u., colony forming units. **b–d**, ETI test in different mutants using *Psm* ES4326/*avrRpt2*. **b**, The hypersensitive response phenotype, 2 and 3 days post inoculation (d.p.i.). **c**, Ion leakage measurement. *rps2*, an *avrRpt2*-insensitive mutant. Error bars represent s.d., $n = 4$. **d**, Growth of *Psm* ES4326/*avrRpt2*. Error bars in **a** and **d** represent 95% confidence intervals, $n = 6$–8. $^{*}P < 0.05$, $^{***}P < 0.001$. **e–g**, Close-up images of an infection site by *Psm* ES4326/*avrRpt2*. Arrows point to intact cells inside the inoculated area. **h**, Image of the whole infection site showing high NPR1(C82A)–GFP accumulation surrounding the PCD zone. The rectangle shows the area from which the close-up images in **e–g** were taken. Yellow staining in **g** and **h** indicates dead cells, green indicates NPR1(C82A)–GFP. Original magnification, ×10 (**e–g**) and ×2 (**h**).

response lesion (Fig. 4h), consistent with the genetic data suggesting that NPR1 is an inhibitor of PCD during ETI.

Discussion

Through this study, we identified the NPR1 paralogues NPR3 and NPR4 as receptors for the immune signal SA. These receptors have different binding affinities to SA (Fig. 3), suggesting that they may be differentially responsive to spatiotemporal changes in cellular SA concentrations. SA controls accessibility of the CUL3 ligase adaptors NPR3 and NPR4 to their substrate NPR1 (Fig. 2), thereby regulating NPR1 stability and activity (Figs 1 and 4).

On the basis of our findings, we present a working model for the regulation of NPR1 by NPR3 and NPR4 in response to different SA levels (Supplementary Fig. 1). In the absence of pathogen challenge, NPR4 constantly removes most of the NPR1 protein by CUL3-NPR4-mediated degradation. This degradation is important to prevent spurious activation of resistance. However, basal SA is required to disrupt some of the NPR1–NPR4 interactions to maintain the basal level of NPR1. This is crucial because SA-deficient plants, *eds5* (ref. 17), *ics1* (also known as *eds16*)[18] and the *nahG* transgenic line expressing an SA-degrading enzyme[19], are impaired in maintaining NPR1 homeostasis (Supplementary Fig. 9), resulting in enhanced disease susceptibility (Supplementary Fig. 1a, b). After challenge by pathogens that trigger ETI, SA levels increase both locally and systemically[20] to form a concentration gradient from the infection site[21,22]. Previous research has shown that high levels of SA facilitate PCD[23,24], and the spread of PCD may be controlled by the activities of proteins such as LSD1 (a zinc-finger protein) and Atrboh D (an NADPH oxidase). Because the *npr3 npr4* double mutant can no longer undergo PCD in response to pathogen effectors, we propose that NPR1, which over-accumulates in the *npr3 npr4* mutant, can act as a negative regulator of PCD. Our finding is in line with a previous report suggesting that NPR1 suppresses hypersensitive response[25]. In support of this function of NPR1, the NPR1–GFP signal is the lowest inside the developing hypersensitive response (Fig. 4e–h) owing to CUL3-NPR3-mediated degradation of NPR1 (Supplementary Fig. 1c). In neighbouring cells, the lower SA level limits NPR1–NPR3 interaction, enabling NPR1 to accumulate in the margin of the hypersensitive response to restrict the spread of PCD and establish SAR (Supplementary Fig. 1d).

METHODS SUMMARY

Protein analysis was carried out as previously described[10]. Total NPR1 protein was detected by an antibody against NPR1. For the *in vitro* degradation assay, the purified recombinant GST–NPR1 was incubated with plant extracts and detected by an anti-GST antibody (GE Healthcare). The *in vitro* pull-down assays for CUL3A, NPR3 and NPR4 were performed using purified recombinant GST–CUL3A and *in vitro* translated NPR3–HA and NPR4–HA, which were detected by an anti-HA antibody (GenScript). Purified recombinant GST–NPR3 and GST–NPR4 proteins retained on the glutathione agarose beads were used to pull down purified His–MBP–NPR1. Bound His–MBP–NPR1 was detected by western blot using an anti-His antibody (GenScript). For co-immunoprecipitation, the immunoprecipitation was performed using an anti-GFP antibody (Abcam) and the western blot using an anti-CUL3A antibody[26] and an anti-GFP antibody (Clontech). Y2H assays were carried out using the Matchmaker system (Clontech). The interactions were determined by yeast growth on selective medium (SD media lacking Trp, Leu and His, plus 3 mM 3-aminotriazole) with or without 100 μM SA, INA or 4-HBA. The SA-binding assays were performed as described[6] with modifications using purified recombinant GST–NPR3 or GST–NPR4 and [^{3}H]-SA (American Radiolabelled Chemicals). Pathogen infection and ion leakage assay using *Psm* ES4326 with or without *avrRpt2* were carried out as previously described[10,27].

Full Methods and any associated references are available in the online version of the paper at www.nature.com/nature.

Received 30 November 2011; accepted 26 April 2012.
Published online 16 May 2012.

1. Jones, J. D. & Dangl, J. L. The plant immune system. *Nature* **444,** 323–329 (2006).
2. Lorrain, S., Vailleau, F., Balague, C. & Roby, D. Lesion mimic mutants: keys for deciphering cell death and defense pathways in plants? *Trends Plant Sci.* **8,** 263–271 (2003).
3. Durrant, W. E. & Dong, X. Systemic acquired resistance. *Annu. Rev. Phytopathol.* **42,** 185–209 (2004).
4. Chen, Z., Silva, H. & Klessig, D. Involvement of reactive oxygen species in the induction of sytemic acquired resistance by salicylic acid in plants. *Science* **262,** 1883–1886 (1993).
5. Park, S. W., Kaimoyo, E., Kumar, D., Mosher, S. & Klessig, D. F. Methyl salicylate is a critical mobile signal for plant systemic acquired resistance. *Science* **318,** 113–116 (2007).
6. Slaymaker, D. H. *et al.* The tobacco salicylic acid-binding protein 3 (SABP3) is the chloroplast carbonic anhydrase, which exhibits antioxidant activity and plays a role in the hypersensitive defense response. *Proc. Natl Acad. Sci. USA* **99,** 11640–11645 (2002).
7. Cao, H., Glazebrook, J., Clark, J. D., Volko, S. & Dong, X. The *Arabidopsis NPR1* gene that controls systemic acquired resistance encodes a novel protein containing ankyrin repeats. *Cell* **88,** 57–63 (1997).
8. Spoel, S. H. & Dong, X. How do plants achieve immunity? Defence without specialized immune cells. *Nature Rev. Immunol.* **12,** 89–100 (2012).
9. Pintard, L., Willems, A. & Peter, M. Cullin-based ubiquitin ligases: Cul3-BTB complexes join the family. *EMBO J.* **23,** 1681–1687 (2004).

10. Spoel, S. H. *et al.* Proteasome-mediated turnover of the transcription coactivator NPR1 plays dual roles in regulating plant immunity. *Cell* **137,** 860–872 (2009).
11. Zhang, Y. *et al.* Negative regulation of defense responses in *Arabidopsis* by two *NPR1* paralogs. *Plant J.* **48,** 647–656 (2006).
12. Santner, A. & Estelle, M. Recent advances and emerging trends in plant hormone signalling. *Nature* **459,** 1071–1078 (2009).
13. Tan, X. *et al.* Mechanism of auxin perception by the TIR1 ubiquitin ligase. *Nature* **446,** 640–645 (2007).
14. Sheard, L. B. *et al.* Jasmonate perception by inositol-phosphate-potentiated COI1-JAZ co-receptor. *Nature* **468,** 400–405 (2010).
15. Métraux, J.-P. *et al.* in *Advances in Molecular Genetics of Plant-Microbe Interactions* Vol. 1 (eds Hennecke, H. & Verma, D. P. S.) 432–439 (Kluwer Academic Publishers, 1991).
16. Mou, Z., Fan, W. & Dong, X. Inducers of plant systemic acquired resistance regulate NPR1 function through redox changes. *Cell* **113,** 935–944 (2003).
17. Nawrath, C., Heck, S., Parinthawong, N. & Métraux, J.-P. EDS5, an essential component of salicylic acid-dependent signaling for disease resistance in *Arabidopsis*, is a member of the MATE transporter family. *Plant Cell* **14,** 275–286 (2002).
18. Wildermuth, M. C., Dewdney, J., Wu, G. & Ausubel, F. M. Isochorismate synthase is required to synthesize salicylic acid for plant defence. *Nature* **414,** 562–565 (2001).
19. Gaffney, T. *et al.* Requirement of salicylic acid for the induction of systemic acquired resistance. *Science* **261,** 754–756 (1993).
20. Malamy, J., Carr, J. P., Klessig, D. F. & Raskin, I. Salicylic acid: a likely endogenous signal in the resistance response of tobacco to viral infection. *Science* **250,** 1002–1004 (1990).
21. Enyedi, A. J., Yalpani, N., Silverman, P. & Raskin, I. Localization, conjugation, and function of salicylic acid in tobacco during the hypersensitive reaction to tobacco mosaic virus. *Proc. Natl Acad. Sci. USA* **89,** 2480–2484 (1992).
22. Dorey, S. *et al.* Spatial and temporal induction of cell death, defense genes, and accumulation of salicylic acid in tobacco leaves reacting hypersensitively to a fungal glycoprotein. *Mol. Plant Microbe Interact.* **10,** 646–655 (1997).
23. Torres, M. A., Jones, J. D. G. & Dangl, J. L. Pathogen-induced, NADPH oxidase-derived reactive oxygen intermediates suppress spread of cell death in *Arabidopsis thaliana*. *Nature Genet.* **37,** 1130–1134 (2005).
24. Lu, H. *et al.* Genetic analysis of *acd6-1* reveals complex defense networks and leads to identification of novel defense genes in *Arabidopsis*. *Plant J.* **58,** 401–412 (2009).
25. Rate, D. N. & Greenberg, J. T. The *Arabidopsis aberrant growth and death2 mutant* shows resistance to *Pseudomonas syringae* and reveals a role for NPR1 in suppressing hypersensitive cell death. *Plant J.* **27,** 203–211 (2001).
26. Dieterle, M. *et al.* Molecular and functional characterization of *Arabidopsis* Cullin 3A. *Plant J.* **41,** 386–399 (2005).
27. Mackey, D., Holt, B. F., Wiig, A. & Dangl, J. L. RIN4 interacts with *Pseudomonas syringae* type III effector molecules and is required for RPM1-mediated resistance in *Arabidopsis*. *Cell* **108,** 743–754 (2002).

Supplementary Information is linked to the online version of the paper at www.nature.com/nature.

Acknowledgements We thank Y. Zhang for sharing the *npr3*, *npr4*, *npr3 npr4* and *npr1 npr3 npr4* mutants; J. Song for providing the NPR3 and NPR4 Y2H constructs; Z. Mou for providing the data on the NPR1–GFP protein levels in the *nahG* transgenic plants, P. Zhou for discussion of the work and for critiquing the manuscript. This work was supported by the Hargitt Fellowship (to Z.Q.F.), grants GM069594-05 (to X.D.), CA107134 (to N.Z.), T32GM008268-23 (to J.R.), Grants-in-Aid for Scientific Research (no. 23120520) from the Ministry of Education, Culture, Sports, Science and Technology of Japan (to Y.T). and the Royal Society Uf090321 (to S.H.S.). N.Z. is a Howard Hughes Medical Institute investigator and X.D. is a Howard Hughes Medical Institute-Gordon and Betty Moore Foundation investigator.

Author Contributions Z.Q.F., S.Y., A.S., R.M. and S.H.S. conceived and discovered that NPR3 and NPR4 mediate NPR1 degradation. Z.Q.F., A.S. and S.Y. found that SA regulates the interactions between the NPR proteins. S.Y., W.W. and A.S. found that NPR3 and NPR4 can bind SA with different affinities. J.R. and N.Z. showed that purified NPR4 recombinant protein exists as a tetramer, which is competent in SA binding. Z.Q.F., W.W. and R.M. demonstrated that the *npr3* and *npr4* single and double mutants are impaired in ETI and SAR. N.O. and Y.T. observed *in situ* accumulation of NPR1(C82A)–GFP in response to *Psm* ES4326/*avrRpt2*. S.H.S. provided data on the detection of NPR1–GFP protein in *eds5* and *ics1* plants. X.D. designed the research and, together with Z.F., S.Y., W.W., S.H.S., A.S. and R.M., wrote the manuscript.

Author Information Reprints and permissions information is available at www.nature.com/reprints. The authors declare no competing financial interests. Readers are welcome to comment on the online version of this article at www.nature.com/nature. Correspondence and requests for materials should be addressed to X.D. (xdong@duke.edu).

METHODS

***Arabidopsis thaliana* mutants and transgenic lines.** *Arabidopsis thaliana* mutants (in ecotype Col-0) *npr3-1*, *npr4-3*, *npr3-1 npr4-3*, *npr1-1 npr3-1 npr4-3*, *npr3-2* (SALK_043055), *npr4-2* (SALK_098460) and *npr3-2 npr4-2* were provided by Y. Zhang[11]. *35S:NPR1-GFP* was introduced into the *npr1-2 npr3-1 npr4-3* background by crossing the *35S:NPR1-GFP* transgenic plants (in *npr1-2*) with the *npr3-1 npr4-3* plants. Homozygous plants were selected by genotyping.

Co-immunoprecipitation assay. Three-week-old plant sample was collected and ground in liquid N_2. Protein was extracted in the extraction buffer (50 mM Tris-HCl, pH 7.5, 150 mM NaCl, 5 mM EDTA, 0.1% Triton X-100, 0.2% Nonidet P-40, and inhibitors: 50 $\mu g\,ml^{-1}$ -*N*-tosyl-L-phenylalanyl chloromethyl ketone (TPCK), 50 $\mu g\,ml^{-1}$ -*N*-tosyl-L-leucine chloromethyl ketone (TLCK), 0.6 mM phenylmethylsulphonyl fluoride (PMSF) and 40 μM MG115). The extracts were then pre-cleared with 50 μl of Dynabeads Protein G (Invitrogen). After 1 μl of anti-GFP antibody (Abcam) was added to the extracts and incubated for 2 h, 50 μl of magnetic Dynabeads was added to the samples and incubated for another hour with gentle rocking. The magnetic Dynabeads were then washed three times using the protein extraction buffer, and bound proteins were eluted by heating the magnetic beads in the SDS sample buffer containing 100 mM DTT at 95 °C for 10 min. The NPR1–GFP and CUL3 proteins were detected by western blotting using an anti-GFP antibody (Clontech) and an anti-CUL3A antibody[26], respectively[10].

Pathogen infection. To test for the hypersensitive response, the avirulent pathogen *Psm* ES4326 carrying *avrRpt2* (attenuance $(D)_{600\,nm} = 0.02$) or *avrRpm1* ($D_{600\,nm} = 0.1$) and *Pst* carrying *avrRps4* ($D_{600\,nm} = 0.1$) or *avrRpt2* ($D_{600\,nm} = 0.02$) were infiltrated into 3–4-week-old leaves. Cell death was recorded 2–3 days after the infiltration. Ion leakage was recorded over time as described[27]. To test for SAR, two lower leaves of 3-week-old plants were pressure-infiltrated with 10 mM $MgCl_2$ or avirulent bacterial pathogen *Psm* ES4326 carrying *avrRpt2* ($D_{600\,nm} = 0.02$). Three days later, virulent bacterial pathogen *Psm* ES4326 ($D_{600\,nm} = 0.001$) was infiltrated into two upper leaves. Disease symptoms were monitored and bacterial growth was analysed 3 days after the inoculation[10].

Imaging of NPR1–GFP in infection site. The *35S:NPR1(C82A)-GFP* plants were inoculated with *Psm* ES4326 carrying *avrRpt2* ($D_{600\,nm} = 0.02$) and incubated for 11 h. Leaf tissues were mounted in 10% glycerol and viewed with a BIOREVO (Keyence) BZ-9000 fluorescence microscope. The GFP signal is monitored with an excitation wavelength of 472.5 nm and a bandpass 502.5 to 537.5 nm emission filter. Red chlorophylls were viewed with an excitation wavelength of 540 nm and a bandpass 573 to 613 nm emission filter. To obtain wide-field view (2 × 5 pictures), image stitching was performed by BZ-II Image Analysis Application. Experiments were repeated eight times.

Molecular cloning of NPRs. The coding regions of *NPR1*, *2*, *3* and *4* were amplified with PrimeSTAR HS DNA polymerase (Takara) using specific primers containing Gateway attB sites (Supplementary Table 1), and then cloned into the pDONR207 entry vector using the BP Clonase (Invitrogen) to create the NPR entry clones. After verification by sequencing, each of the clones was mobilized using the LR Clonase (Invitrogen) into the Gateway destination vectors pDEST-GBKT7 and pDEST-GADT7 for yeast transformation[28], the protein expression vectors pDEST15 (Invitrogen) and pDEST-HisMBP (Addgene plasmid 11085)[29] for making the GST and His–MBP fusions, respectively.

Detection of the NPR1 protein. Four-week-old plants were sprayed with 0.5 mM SA and collected at different time points. Total protein was extracted in a buffer containing 50 mM Tris-HCl, pH 7.5, 150 mM NaCl, 5 mM EDTA, 0.1% Triton X-100, 0.2% Nonidet P-40, and inhibitors: 50 $\mu g\,ml^{-1}$ TPCK, 50 $\mu g\,ml^{-1}$ TLCK, 0.6 mM PMSF and 40 μM MG115 (ref. 30). The homogenates were centrifuged twice at 13,500*g* for 15 min each. Protein was denatured in the SDS sample buffer containing 100 mM DTT at 75 °C for 10 min, and western blot analysis was performed using an antibody against NPR1 (ref. 16).

Quantitative real-time PCR. Total RNA was extracted from 4-week-old control and SA-treated plants at the indicated time points using TRIzol Reagent (Invitrogen). Genomic DNA was eliminated by treatment of the RNA with 2 U of TURBO DNA-free (Ambion). cDNA was synthesized using the Superscript III Reverse Transcription kit (Invitrogen) and analysed by quantitative real-time PCR using the FastStart Universal SYBR Green Master (Rox) kit (Roche) with gene-specific primers for *NPR1* and *ubiquitin 5* (Supplementary Table 1).

***In vitro* degradation assay.** The NPR1 degradation assay was performed as described[10]. Leaves from wild-type or *npr3-1 npr4-3* double mutant plants were ground in liquid N_2 and resuspended in the proteolysis buffer containing 25 mM Tris-HCl, pH 7.5, 10 mM $MgCl_2$, 10 mM NaCl, 10 mM ATP and 5 mM DTT. After centrifugation, the supernatants were mixed with the GST–NPR1 protein purified from *Escherichia coli* and incubated at room temperature for 15 min. The reactions were stopped by adding the SDS sample buffer containing 100 mM DTT and incubated at 75 °C for 10 min. The level of GST–NPR1 protein was analysed by western blotting using an anti-GST antibody (GE Healthcare).

***In vitro* pull-down assay.** The coding sequence of *CUL3A* was cloned into the GST vector pGEX4T-2 (GE Healthcare) for expression in *E. coli* BL21(DE3). The coding sequences of *NPR3* and *NPR4* were cloned into pCMX-PL2 for *in vitro* translation using TNT Quick Coupled Transcription/Translation System (Promega) to produce the HA-tagged NPR3 and NPR4 proteins. The purified GST–CUL3A protein was bound to the glutathione agarose beads, incubated with the HA-tagged NPR3 or NPR4 protein, and washed three times with EB buffer (50 mM Tris-HCl, pH 7.2, 100 mM NaCl, 1 mM EDTA, 1 mM EGTA, 1% dimethylsulphoxide, 20 mM DTT and 0.1% NP40). The HA-tagged NPR3 or NPR4 protein bound to GST–CUL3A protein was detected by western blot analysis using an anti-HA antibody (GenScript). Recombinant His-MBP-tagged NPR1 and GST-tagged NPR3 and NPR4 proteins were produced in *E. coli*. The recombinant His-MBP-tagged NPR1 was purified using the Ni-NTA resin (QIAGEN). GST-tagged NPR3 and NPR4 proteins were purified using glutathione beads and retained on the beads to pull down purified His–MBP–NPR1 protein with or without 100 μM SA in a buffer containing 50 mM Tris-HCl, pH 6.8, 100 mM NaCl and 0.1% NP40. After washing three times, bound His–MBP–NPR1 was eluted by heating the glutathione beads at 95 °C for 10 min in the SDS buffer with 100 mM DTT and detected by western blot analysis using an anti-His antibody (GenScript). Equal loadings were verified by staining the membrane with Ponceau S.

Yeast two-hybrid assay. The *Saccharomyces cerevisiae* yeast strains AH109 and Y187 were transformed with pGADT7-NPR1, 2, 3, 4 and pGBKT7-NPR1, 2, 3, 4, respectively, according to the Clontech yeast transformation protocol. Yeast strains were grown on SD−Trp−Leu plates, and then fresh single colonies were grown for 1 day in the SD−Trp−Leu liquid media. Interactions between bait and prey were detected on the selective media: SD−Trp−Leu−His (control), SD−Trp−Leu−His with 100 μM sodium salicylate (SA), 100 μM INA, or 100 μM 4-HBA. All of the SD−Trp−Leu−His selective media also contained 3 mM 3-aminotriazole.

SA-binding assay. The SA-binding assay was performed as described[6] with modifications. The GST–NPR3 and GST–NPR4 proteins were expressed in *E. coli* C41 and purified using Pierce Glutathione Magnetic Beads (Thermo). The protein-bound beads were incubated in 100 μl buffer containing 30 mM sodium citrate, pH 6.3, 1 mM EDTA and [^{3}H]-SA (American Radiolabelled Chemicals, specific activity 30 Ci $mmol^{-1}$). The beads were washed twice, resuspended in 100 μl H_2O, mixed with 6 ml Ultima Gold Cocktails (PerkinElmer) and counted using the LC6000SC liquid scintillation counter (Beckman Instruments). The non-specific binding was determined in the presence of 1 mM unlabelled SA. The data were analysed using GraphPad Prism 5.

Gel filtration analyses of NPR4. NPR4 was overexpressed as a GST-fusion protein in insect cells and purified by glutathione affinity chromatography in the presence of 100 mM DTT. After TEV cleavage, NPR4 was further purified by anion exchange chromatography and dialysed against a buffer containing 20 mM Tris-HCl, pH 8.0, 200 mM NaCl and 5 mM DTT. After concentration, 0.5–1 mg NPR4 was analysed in the same buffer with and without 10 μM SA as indicated by size exclusion chromatography on a Supderdex 200 gel filtration column. Co-elution of SA and NPR4 was monitored by [^{3}H]-SA, which was pre-mixed with the NPR4 protein before injection.

28. Rossignol, P., Collier, S., Bush, M., Shaw, P. & Doonan, J. H. *Arabidopsis* POT1A interacts with TERT-V(I8), an N-terminal splicing variant of telomerase. *J. Cell Sci.* **120,** 3678–3687 (2007).
29. Nallamsetty, S., Austin, B. P., Penrose, K. J. & Waugh, D. S. Gateway vectors for the production of combinatorially-tagged His6-MBP fusion proteins in the cytoplasm and periplasm of *Escherichia coli*. *Protein Sci.* **14,** 2964–2971 (2005).
30. Fan, W. & Dong, X. *In vivo* interaction between NPR1 and transcription factor TGA2 leads to salicylic acid-mediated gene activation in *Arabidopsis*. *Plant Cell* **14,** 1377–1389 (2002).